HHS Public Access

Author manuscript

Curr Opin Struct Biol. Author manuscript; available in PMC 2020 October 01.

Published in final edited form as:

Curr Opin Struct Biol. 2019 October ; 58: 224–232. doi:10.1016/j.sbi.2019.05.001.

Enabling technologies in super-resolution fluorescence microscopy: Reporters, labeling, and methods of measurement

Alecia Marie Achimovich[a], **Huiwang Ai**[a,b], **Andreas Gahlmann**[a,b,#]

[a]Department of Molecular Physiology & Biological Physics, University of Virginia School of Medicine, Charlottesville, Virginia, USA

[b]Department of Chemistry, University of Virginia, Charlottesville, Virginia, USA

Abstract

Super-resolution fluorescence microscopy continues to experience a period of extraordinary development. New instrumentation and fluorescent labeling strategies provide access to molecular and cellular processes that occur on length scales ranging from nanometers to millimeters and on time scales ranging from milliseconds to hours. At the shortest length scales, single-molecule imaging methods now allow measurement of nanoscale localization, motion, and binding kinetics of individual biomolecules. At cellular and intercellular length scales, super-resolution microscopy allows structural and functional imaging of individual cells in tissues and even in whole animals. Here, we review recent advances that have enabled entirely new types of experiments and greatly potentiated existing technologies.

Introduction

The fluorescence microscope is a mainstay instrument in cell biology due to its unique ability to visualize fluorescently-labeled molecules and cellular structures with unsurpassed specificity and contrast. Importantly, fluorescence microscopy is compatible with live-cell imaging, which enables the determination of spatial distributions of biomolecules in their native environment. Fluorescence microscopy thus provides a crucial complement to other whole-cell imaging technologies, such as electron and X-ray cryo-tomography, which can achieve 2–50 nm resolution [1–3]. The spatial resolution of conventional fluorescence microscopes, as defined by Ernst Abbe, is fundamentally limited by diffraction to roughly one half of the optical wavelength [4]. For visible light, the resolution is thus limited to 250–300 nm, which is too coarse to resolve biological events that occur at length scales of a few nanometers. To surpass this barrier, the last two decades has been marked by continuing developments of super-resolution fluorescence microscopy modalities, including stimulated emission depletion (STED) [5], (fluorescence) photo-activated localization microscopy

[#]Address correspondence to Andreas Gahlmann, agahlmann@virginia.edu.

The authors declare no conflict of interest.

((F)PALM) [6,7], stochastic optical reconstruction microscopy (STORM) [8], super-resolution optical fluctuation imaging (SOFI) [9,10], and MINFLUX microscopy [11], which all circumvent the optical diffraction limit through different mechanisms (Figure 1). These methods provide access to nanoscale spatial information in living and fixed biological specimens – a feat that had remained elusive for optical microscopy for well over a century. Super-resolution microscopy now enables researchers to zoom in further, and resolve the molecular and cellular underpinnings of life with unprecedented specificity, sensitivity, and resolution.

In the era of super-resolution microscopy, the achievable spatial and temporal resolutions and overall information content in the obtained images are fundamentally limited by the physical and chemical properties of the fluorophores, as well as the labeling strategies used to target them to specific biomolecules and cellular structures. The fluorophores take center-stage because optical imaging below the diffraction limit relies on the fact that fluorescent molecules can switch repeatedly between fluorescent ON or non-fluorescent OFF states (Figure 1). Even so, achieving optimal super-resolution imaging in intact cells, tissues, or even whole animals has required the development of new and improved instrumentation. Here, we discuss a few key examples of enabling developments in recent years that have potentiated existing technologies and provided entirely new measurement capabilities.

Improvements for single-molecule localization and tracking microscopy

The goal of PALM/STORM-type single-molecule localization and tracking experiments is to determine the positions of individual, fluorescently-labeled biomolecules as accurately and precisely as possible without perturbing their native function (Figure 1a). In practice, the properties of the fluorescent tag (i.e. its size, brightness, photostability), the labeling strategy (i.e. efficiency, specificity, and live-cell compatibility), and optical aberrations in the imaging system stand in the way of this goal. For example, fluorescent proteins continue to be the preferred labels for live-cell imaging, because they can be expressed by the cells themselves and genetically targeted to the proteins of interest with an efficiency and specificity that has not yet been matched by chemical labeling strategies [12]. However, the reduced brightness and photostability of fluorescent proteins compared to most chemical dyes has been a major limitation, as the limited photon budget results in reduced localization precisions and short observation times.

The use of relatively dim fluorescent proteins for live-cell single-molecule imaging and tracking experiments has been greatly potentiated by the recent development of MINFLUX microscopy [11] (Figure 1c). MINFLUX is a new localization scheme that converts photon information much more efficiently than camera-based tracking (PALM/STORM). Excitation light with an intensity minimum at its center, similar to the doughnut beam used in STED (Figure 1b), is targeted to known positions around a single fluorophore (compare Figures 1a, b and c). The numbers of emitted photons at each doughnut position are then used to calculate the position of the fluorophore. For stationary fluorophores, MINFLUX microscopy can achieve < 2 nm localization precisions using only 500 photons, thus reaching molecular resolution with single molecule fluorophores and surpassing the performance of camera-based localization schemes used in PALM by an order of magnitude.

Compared to camera-based tracking of moving emitters, MINFLUX provides single-molecule trajectories containing an order of magnitude more localizations (hundreds vs. tens), and each trajectory is sampled at one to two orders of magnitude higher time resolution (200 μs vs. 2–20 ms).

For MINFLUX tracking the doughnut minimum has to be kept near the continuously moving fluorophore. Thus, frequent position sampling, i.e. high time resolution, is required to avoid losing moving molecules. To achieve a time resolution of 200 μs using 12 fluorescent photons per localization event, the *detected* fluorescent photon count rate has to be around 75 kHz. Such count rates were possible using the fluorescent protein mEos2 in the initial demonstration of MINFLUX [11]. A time resolution of 200 μs was sufficient to track slowly diffusing ($D < 2\ \mu m^2/s$) 30S ribosomal subunit proteins in *E. coli*. For tracking of faster moving molecules, either the emission count rate of the fluorophore or the size of the scan range L has to be increased. The latter measure lowers the localization precision at each time point. Thus, MINFLUX microscopy, like camera-based localization methods, encounters a fluorophore-limited trade-off between spatial and temporal resolution, albeit at much more favorable values. In a recent demonstration of MINFLUX tracking, the DNA-tethered dye ATTO647N yielded a count rate of 350 kHz, when excited slightly below its excitation saturation threshold [13]. It is therefore highly desirable to develop bright photo-activatable or photo-switchable fluorescent protein and dye labels that can achieve count rates close to 1 MHz (required for 20 μs time resolution). The emission count rate of currently available fluorescent dyes and proteins is primarily limited by repeated transitions to non-fluorescent dark states [14] a property of fluorophores that is undesirable for single-molecule microscopy, but exploited in super-resolution optical fluctuation imaging (SOFI) [9,10] (Figure 1d).

PALM and MINFLUX microscopy rely on sequential photo-activation to ensure that single molecules can be probed individually. An alternative approach to achieve low concentrations of actively emitting fluorophores is to label only a small subset of expressed proteins using stochastic protein labeling [15]. Stochastic protein labeling is achieved by flanking the stop codon of the gene of interest with two unique 3-letter nucleotide sequences immediately upstream of the gene for a fluorescent tag. By use of these gene sequences, ribosome stop codon read-through occurs with low-probability (<0.1%), such that only a small subset of the expressed proteins will be fused to the fluorescent tag. The fluorescence signal can be amplified by using multivalent tags, such as the Sun-tag [16] or the 3x-HALO repeat [17], combined with bright fluorophores, such as Janelia Fluor dyes [18]. More recently, exchange of fluorogenic probes in epitope arrays has been exploited to provide unbleachable fluorescent labels [19]. Signal amplification using array tags enables higher localization precisions and/or longer trajectories in PALM/STORM or MINFLUX-based tracking, but also increases the overall molecular mass of the fluorescent label (1–2.5 MDa vs. 27 kDa for a single fluorescent protein).

Super-resolution imaging biomolecular activity in living cells

The research fields of fluorescence-based biosensing [20,21] and super-resolution imaging have remained largely separate. While super-resolution microscopy offers information about

the nanoscale locations of fluorescently-labeled biomolecules, the biochemical activity of the tagged molecules cannot be simultaneously inferred. Recently however, Mo et al. bridged this gap by introducing a new class of biosensors that enable readouts of enzymatic activity at spatial resolutions below the optical diffraction limit [22]. These biosensors, modeled after similar FRET-based biosensors [20], rely on the newly discovered phenomenon that the proximity of two fluorescent proteins (in this case Dronpa and TagRFP-T) can alter the fluorescence fluctuation rates of TagRFP-T. The fluorescence fluctuation rates change over an effective distance of 5–6 nm, and these changes are quantifiable through photochromic Stochastic Optical Fluctuation Imaging (pcSOFI, Figure 2) [23]. The resulting pcSOFI images provide the spatial positioning of TagRFPT *and* a measure of the proximity between TagRFP-T and Dronpa, i.e., the signaling state of the biosensor. This new approach, termed FLuctuation INcrease by Contact (FLINC), was validated in living cells by using Protein Kinase A (PKA) activity as a test case. PKA is a signaling protein that phosphorylates downstream proteins in response to G-protein coupled receptor activation. A PKA-specific substrate peptide linked to a phosphoamino-acid-binding domain (PAABD) was tagged with TagRFP-T and Dronpa, resulting in a FLINC-based A-Kinase Activity Reporter (FLINC-AKAR1) (Figure 2a). Hotspots of PKA activity were detected at the plasma membrane when both labels were in close proximity, which resulted in a spatially localized FLINC signal (Figure 2b). As with FRET-based biosensing, the distance sensitivity of FLINC makes this new class of biosensors generally applicable to a wide-variety of biological processes, including localized enzyme activities and ion concentrations in cells [20,24–26].

Capturing the big picture: High-content super-resolution imaging

Large scale “–omics” studies have been very successful in providing population-averaged transcriptomic, proteomic, and metabolomic profiles of cells and tissues. However, cell heterogeneity and rare subpopulations remain undetectable with these techniques. Recent efforts have therefore focused on using super-resolution microscopy to spatially map and quantify the distributions of proteins and RNA transcripts in single cells. Key challenges for this endeavor are the large numbers of targets to image and the limited number of resolvable fluorescent wavelengths in the visible spectrum. In other words, fluorescence microscopy is not readily parallelizable to enable simultaneous imaging of hundreds of targets in single cells. Therefore, visual proteomics and transcriptomics with (sub-)cellular resolution requires sequential labeling and imaging of the specimen.

Recent extensions to the Points Accumulation for Imaging in Nanoscale Topography (PAINT) [27–30] technique have been particularly promising for mapping the spatial localizations of tens and possibly hundreds of proteins in single cells. In DNA PAINT, antibodies modified with short DNA nucleotides bind to proteins of interest within fixed and permeabilized cells [31]. Dyeconjugated DNA strands, so called imager stands, are then introduced into the sample (Figure 3a). Before binding to the complementary DNA sequence on the antibody, imager strands diffuse rapidly, so that their fluorescence emission contributes to a diffuse cellular fluorescence background. Once bound, however, the imager strands produce sharp point-spread-functions enabling their localization. Localized signal detection upon binding replaces fluorophore photoactivation and blinking used in PALM and

STORM (Figure 1a). In contrast to covalent labeling strategies, DNA-PAINT imaging enables theoretically unlimited localizations of the same protein through turnover of reversibly bound imager strands. Furthermore, the fluorophore binding kinetics can be controlled by adjusting the imager strand concentration and the binding affinity can be controlled by changing DNA strand length and degree of complementarity. However, the use of high concentrations of unbound imager strands also increases the diffuse background signal. To improve the signal-to-background ratio, Förster resonance energy transfer (FRET)-based imager strands have been developed recently [32,33]. In FRET-PAINT, the imager and docking strands are respectively labeled with donor and acceptor dyes. A FRET signal from the acceptor dye on the docking strand will only be detected upon binding of an imager strand (Figure 3a). By monitoring the red-shifted FRET signal, the signal-to-background ratio is improved dramatically so that higher concentrations of imager strands can be used. FRET-PAINT enabled an increase in imager strand concentration by two orders or magnitude, while maintaining a similar signal-to-background ratio as conventional DNA-PAINT. The accompanying increase in imager strand binding events cut down the total data acquisition time by a factor of 30. Finally, exchange-PAINT (Figure 3a) enables probing of 8–10 different protein targets by sequentially introducing and then washing out different imager strands with different DNA complementarities [34–36]. Since binding events are transient by design, exchange-PAINT enables faster washing and relabeling compared to immuno-labeling approaches. The exchange-PAINT principle is fully compatible with FRET-based imager probes, which could further increase data acquisition throughput and enable imaging of hundreds of different proteins in the same cell.

Similar strategies have also led to breakthroughs in imaging-based transcriptomics. Multiplexed, error-robust fluorescence *in-situ* hybridization (MERFISH) [37] utilizes single-molecule FISH (smFISH) [38,39] to localize and identify RNA transcripts in single cells. Specifically-designed encoding probes stably bind to RNA transcripts through base pair complementarity. These encoding probes are flanked by a unique combination of read-out sequences that act as high-affinity docking sites for STORM dye-labeled RNA imager strands. As in exchange-PAINT, imager strands are sequentially introduced, spatially localized by STORM, and then the attached dye is photobleached or chemically cleaved to enable the next round of imaging. Through the use of L different imager strands in N rounds of imaging, each RNA transcript can be precisely localized and identified by a unique barcode, corresponding to whether the encoding probe was labeled with an imager strand in a given round of imaging (Figure 3b). By integrating MERFISH with two-color imaging and automating data acquisition, over 100 RNAs in ~40,000 cells could be identified [40]. Thus, MERFISH imaging achieved data acquisition throughputs comparable to droplet-based, single-cell sequencing approaches [41–43], with the additional advantage of providing the subcellular locations of the imaged RNA transcripts within each cell. MERFISH thus enables the detection of spatially correlated RNA profiles within a cell population. For example, the technique successfully identified dividing cells by detecting up-regulation of genes encoding the cell-division machinery. Neighboring cells exhibited similar levels of up-regulation, suggesting a level of synchronization due to a common recent progenitor cell or the presence of local environmental signals.

The DNA- and RNA-based imaging methods described above provide spatial information about hundreds of protein and RNA targets in the populations of cells. However, the sequential labeling and washing steps that enable these capabilities limit these techniques to static imaging of fixed cells. Capturing molecular and cellular behaviors in real time requires live-cell compatible labeling and imaging approaches. Lattice-light sheet microscopy (LLSM) is perhaps the most versatile live-cell imaging platform capable of probing the 3D dynamics of cells and cellular organelles with high spatial and temporal resolution [44]. Spatial structuring of excitation light into thin optical lattices enables super-resolution imaging through structured illumination microscopy (SIM) [45,46]. Perhaps more importantly, the perpendicular excitation and detection geometry enables noninvasive long-term imaging of light-sensitive specimens. Since its initial demonstration in 2014, Betzig and co-workers have continued to refine LLSM to push its spatial resolution [47], as well as its multicolor [48], and deep-tissue imaging capabilities [49]. Patterned activation followed by patterned excitation of the reversible photo-switchable fluorescent protein Skylan-NS [50] achieved 120 × 230 × 170 nm 3D spatial resolution [47] through non-linear structured illumination microscopy (NL-SIM) [51]. In a separate effort, LLSM was implemented with 6 different excitation wavelengths and 4 different detection channels to achieve 6-color imaging after linear unmixing [48,52]. Multicolor LLSM provided unprecedented 5-dimensional datasets (3 spatial dimensions, time, and wavelength) that begin to capture the full complexity of organelle motion and interplay in living cells. The combination of LLSM with protein-retention expansion microscopy [53,54] enabled multicolor fluorescence imaging of the complete Drosophila brain at 60 × 60 × 90 nm resolution in under 100 hours [55]. Recently, the capabilities of LLSM were further improved through the use of adaptive optical elements (AO-LLSM) that compensate for optical aberrations induced by refractive index mismatches in thick biological specimens [49]. Spatial light modulators and deformable mirrors in the excitation and emission beam paths enabled diffraction-limited imaging of cells deeply embedded in tissues and living animals (Figure 4). The combination of these technologies in a single instrument paves the way towards super-resolution imaging of cellular structures and cellular dynamics, as they occur in their native 3-dimensional environment.

Conclusion

Super-resolution microscopy continues to benefit from paradigm-shifting developments of novel measurements technologies, fluorescent labeling strategies, and functional imaging probes. Here, we highlighted a few key examples in each of these categories that have enabled experimental access to previously inaccessible biological processes within cells. These developments now set the stage for mapping the structure and the activity architecture of cells, cellular organelles, and individual molecules. Experiments using super-resolution microscopy continue to benefit from the development of ever more powerful gene-editing technologies [56–58] and from experimental tools that enable chemical or real-time optical manipulation of bimolecular activity in living cells [59,60]. Given the long and successful track record of fluorescence microscopy in elucidating the functional properties of biological systems, the ongoing technological advances in super-resolution fluorescence microscopy

will undoubtedly continue to transform our understanding of life at the smallest length scales.

Acknowledgements

We thank all members of the Gahlmann and Ai Labs for fruitful discussions. This work is supported in part by U.S. National Institutes of Health Grant R01GM118675 to H.A. A.A. is supported in part by the U.S. National Institutes of Health Grant 5T32GM080186–08.

References

1. Harkiolaki M, Darrow MC, Spink MC, Kosior E, Dent K, Duke E: Cryo-soft X-ray tomography: using soft X-rays to explore the ultrastructure of whole cells. Emerging Topics in Life Sciences 2018, 2:81–92.
2. Oikonomou CM, Jensen GJ: A new view into prokaryotic cell biology from electron cryotomography. Nat Rev Microbiol 2016, 14:205–220. [PubMed: 26923112]
3. Ekman AA, Chen JH, Guo J, McDermott G, Le Gros MA, Larabell CA: Mesoscale imaging with cryo-light and X-rays: Larger than molecular machines, smaller than a cell. Biol Cell 2017, 109:24–38. [PubMed: 27690365]
4. Abbe E: Beiträge zur Theorie des Mikroskops und der mikroskopischen Wahrnehmung. Archiv für mikroskopische Anatomie 1873, 9:413–418.
5. Hell SW, Wichmann J: Breaking the diffraction resolution limit by stimulated-emission - stimulated-emission-depletion fluorescence microscopy. Optics Letters 1994, 19:780–782. [PubMed: 19844443]
6. Hess ST, Girirajan TPK, Mason MD: Ultra-high resolution imaging by fluorescence photoactivation localization microscopy. Biophysical Journal 2006, 91:4258–4272. [PubMed: 16980368]
7. Betzig E, Patterson GH, Sougrat R, Lindwasser OW, Olenych S, Bonifacino JS, Davidson MW, Lippincott-Schwartz J, Hess HF: Imaging intracellular fluorescent proteins at nanometer resolution. Science 2006, 313:1642–1645. [PubMed: 16902090]
8. Rust MJ, Bates M, Zhuang XW: Sub-diffraction-limit imaging by stochastic optical reconstruction microscopy (STORM). Nature Methods 2006, 3:793–795. [PubMed: 16896339]
9. Dertinger T, Colyer R, Iyer G, Weiss S, Enderlein J: Fast, background-free, 3D super-resolution optical fluctuation imaging (SOFI). Proceedings of the National Academy of Sciences of the United States of America 2009, 106:22287–22292. [PubMed: 20018714]
10. Dertinger T, Colyer R, Vogel R, Enderlein J, Weiss S: Achieving increased resolution and more pixels with Superresolution Optical Fluctuation Imaging (SOFI). Optics Express 2010, 18:18875–18885. [PubMed: 20940780]
11. Balzarotti F, Eilers Y, Gwosch KC, Gynnå AH, Westphal V, Stefani FD, Elf J, Hell SW: Nanometer resolution imaging and tracking of fluorescent molecules with minimal photon fluxes. Science 2017, 355:606–612. [PubMed: 28008086]
12. Gahlmann A, Moerner WE: Exploring bacterial cell biology with single-molecule tracking and super-resolution imaging. Nature Reviews Microbiology 2014, 12:9–22. [PubMed: 24336182]
13. Eilers Y, Ta H, Gwosch KC, Balzarotti F, Hell SW: MINFLUX monitors rapid molecular jumps with superior spatiotemporal resolution. Proc Natl Acad Sci U S A 2018.
14. Pennacchietti F, Gould TJ, Hess ST: The Role of Probe Photophysics in Localization-Based Superresolution Microscopy. Biophysical Journal 113:2037–2054.
15. Liu H, Dong P, Ioannou MS, Li L, Shea J, Pasolli HA, Grimm JB, Rivlin PK, Lavis LD, Koyama M, et al.: Visualizing long-term single-molecule dynamics in vivo by stochastic protein labeling. Proc Natl Acad Sci U S A 2018, 115:343–348. [PubMed: 29284749]
16. Tanenbaum ME, Gilbert LA, Qi LS, Weissman JS, Vale RD: A protein-tagging system for signal amplification in gene expression and fluorescence imaging. Cell 2014, 159:635–646. [PubMed: 25307933]

17. Los GV, Encell LP, McDougall MG, Hartzell DD, Karassina N, Zimprich C, Wood MG, Learish R, Ohana RF, Urh M, et al.: HaloTag: A Novel Protein Labeling Technology for Cell Imaging and Protein Analysis. ACS Chemical Biology 2008, 3:373–382. [PubMed: 18533659]
18. Grimm JB, English BP, Choi H, Muthusamy AK, Mehl BP, Dong P, Brown TA, Lippincott-Schwartz J, Liu Z, Lionnet T, et al.: Bright photoactivatable fluorophores for single-molecule imaging. Nat Methods 2016, 13:985–988. [PubMed: 27776112]
19. Ghosh RP, Franklin JM, Draper WE, Shi Q, Beltran B, Spakowitz AJ, Liphardt JT: A fluorogenic array for temporally unlimited single-molecule tracking. Nat Chem Biol 2019, 15:401–409. [PubMed: 30858596]
20. Newman RH, Fosbrink MD, Zhang J: Genetically encodable fluorescent biosensors for tracking signaling dynamics in living cells. Chem Rev 2011, 111:3614–3666. [PubMed: 21456512]
21. Medintz I, Hildebrandt N: FRET - Förster Resonance Energy Transfer : From Theory to Applications. Edited by: John Wiley & Sons, Incorporated; 2013:269–278.
22. Mo GC, Ross B, Hertel F, Manna P, Yang X, Greenwald E, Booth C, Plummer AM, Tenner B, Chen Z, et al.: Genetically encoded biosensors for visualizing live-cell biochemical activity at super-resolution. Nat Methods 2017, 14:427–434. [PubMed: 28288122]
23. Dedecker P, Mo GC, Dertinger T, Zhang J: Widely accessible method for superresolution fluorescence imaging of living systems. Proc Natl Acad Sci U S A 2012.
24. Ai HW: Fluorescent-protein-based probes: general principles and practices. Anal Bioanal Chem 2015, 407:9–15. [PubMed: 25326886]
25. Aoki K, Kamioka Y, Matsuda M: Fluorescence resonance energy transfer imaging of cell signaling from in vitro to in vivo: basis of biosensor construction, live imaging, and image processing. Dev Growth Differ 2013, 55:515–522. [PubMed: 23387795]
26. Campbell RE: Fluorescent-Protein-Based Biosensors: Modulation of Energy Transfer as a Design Principle. Analytical Chemistry 2009, 81:5972–5979. [PubMed: 19552419]
27. Sharonov A, Hochstrasser RM: Wide-field subdiffraction imaging by accumulated binding of diffusing probes. Proceedings of the National Academy of Sciences 2006, 103:18911–18916.
28. Lew MD, Lee SF, Ptacin JL, Lee MK, Twieg RJ, Shapiro L, Moerner WE: Three-dimensional superresolution colocalization of intracellular protein superstructures and the cell surface in live Caulobacter crescentus. Proceedings of the National Academy of Sciences of the United States of America 2011, 108:E1102–E1110. [PubMed: 22031697]
29. Gahlmann A, Ptacin JL, Grover G, Quirin S, von Diezmann ARS, Lee MK, Backlund MP, Shapiro L, Piestun R, Moerner WE: Quantitative Multicolor Subdiffraction Imaging of Bacterial Protein Ultrastructures in Three Dimensions. Nano Letters 2013, 13:987–993. [PubMed: 23414562]
30. Legant WR, Shao L, Grimm JB, Brown TA, Milkie DE, Avants BB, Lavis LD, Betzig E: High-density three-dimensional localization microscopy across large volumes. Nat Methods 2016, 13:359–365. [PubMed: 26950745]
31. Jungmann R, Steinhauer C, Scheible M, Kuzyk A, Tinnefeld P, Simmel FC: Single-molecule kinetics and super-resolution microscopy by fluorescence imaging of transient binding on DNA origami. Nano Lett 2010, 10:4756–4761. [PubMed: 20957983]
32. Auer A, Strauss MT, Schlichthaerle T, Jungmann R: Fast, Background-Free DNA-PAINT Imaging Using FRET-Based Probes. Nano Lett 2017, 17:6428–6434. [PubMed: 28871786]
33. Lee J, Park S, Kang W, Hohng S: Accelerated super-resolution imaging with FRET-PAINT. Mol Brain 2017, 10:63. [PubMed: 29284498]
34. Jungmann R, Avendano MS, Woehrstein JB, Dai M, Shih WM, Yin P: Multiplexed 3D cellular super-resolution imaging with DNA-PAINT and Exchange-PAINT. Nat Methods 2014, 11:313–318. [PubMed: 24487583]
35. Wang Y, Woehrstein JB, Donoghue N, Dai M, Avendano MS, Schackmann RCJ, Zoeller JJ, Wang SSH, Tillberg PW, Park D, et al.: Rapid Sequential in Situ Multiplexing with DNA Exchange Imaging in Neuronal Cells and Tissues. Nano Lett 2017, 17:6131–6139. [PubMed: 28933153]
36. Agasti SS, Wang Y, Schueder F, Sukumar A, Jungmann R, Yin P: DNA-barcoded labeling probes for highly multiplexed Exchange-PAINT imaging. Chem Sci 2017, 8:3080–3091. [PubMed: 28451377]

37. Chen KH, Boettiger AN, Moffitt JR, Wang S, Zhuang X: RNA imaging. Spatially resolved, highly multiplexed RNA profiling in single cells. Science 2015, 348:aaa6090. [PubMed: 25858977]
38. Raj A, van den Bogaard P, Rifkin SA, van Oudenaarden A, Tyagi S: Imaging individual mRNA molecules using multiple singly labeled probes. Nat Methods 2008, 5:877–879. [PubMed: 18806792]
39. Femino AMF, Frederic S.; Fogarty, Kevin; Singer, Robert H. : Visualization of single RNA transcripts in situ. Science 1998, 280:585–590. [PubMed: 9554849]
40. Moffitt JR, Zhuang X: RNA Imaging with Multiplexed Error-Robust Fluorescence In Situ Hybridization (MERFISH). Methods Enzymol 2016, 572:1–49. [PubMed: 27241748]
41. Gawad C, Koh W, Quake SR: Single-cell genome sequencing: current state of the science. Nat Rev Genet 2016, 17:175–188. [PubMed: 26806412]
42. Klein AM, Mazutis L, Akartuna I, Tallapragada N, Veres A, Li V, Peshkin L, Weitz DA, Kirschner MW: Droplet barcoding for single-cell transcriptomics applied to embryonic stem cells. Cell 2015, 161:1187–1201. [PubMed: 26000487]
43. Macosko EZ, Basu A, Satija R, Nemesh J, Shekhar K, Goldman M, Tirosh I, Bialas AR, Kamitaki N, Martersteck EM, et al.: Highly Parallel Genome-wide Expression Profiling of Individual Cells Using Nanoliter Droplets. Cell 2015, 161:1202–1214. [PubMed: 26000488]
44. Chen BC, Legant WR, Wang K, Shao L, Milkie DE, Davidson MW, Janetopoulos C, Wu XS, Hammer JA 3rd, Liu Z, et al.: Lattice light-sheet microscopy: imaging molecules to embryos at high spatiotemporal resolution. Science 2014, 346:1257998. [PubMed: 25342811]
45. Gustafsson MGL: Surpassing the lateral resolution limit by a factor of two using structured illumination microscopy. Journal of Microscopy 2000, 198:82–87. [PubMed: 10810003]
46. Heintzmann R, Huser T: Super-Resolution Structured Illumination Microscopy. Chemical Reviews 2017.
47. Li D, Shao L, Chen BC, Zhang X, Zhang M, Moses B, Milkie DE, Beach JR, Hammer JA 3rd, Pasham M, et al.: Extended-resolution structured illumination imaging of endocytic and cytoskeletal dynamics. Science 2015, 349:aab3500. [PubMed: 26315442]
48. Valm AM, Cohen S, Legant WR, Melunis J, Hershberg U, Wait E, Cohen AR, Davidson MW, Betzig E, Lippincott-Schwartz J: Applying systems-level spectral imaging and analysis to reveal the organelle interactome. Nature 2017, 546:162–167. [PubMed: 28538724]
49. Liu T-L, Upadhyayula S, Milkie DE, Singh V, Wang K, Swinburne IA, Mosaliganti KR, Collins ZM, Hiscock TW, Shea J, et al.: Observing the cell in its native state: Imaging subcellular dynamics in multicellular organisms. Science 2018, 360: eaaq1392. [PubMed: 29674564]
50. Zhang X, Zhang M, Li D, He W, Peng J, Betzig E, Xu P: Highly photostable, reversibly photoswitchable fluorescent protein with high contrast ratio for live-cell superresolution microscopy. Proceedings of the National Academy of Sciences 2016, 113:10364–10369.
51. Gustafsson MGL: Nonlinear structured-illumination microscopy: Wide-field fluorescence imaging with theoretically unlimited resolution. Proceedings of the National Academy of Sciences 2005, 102:13081–13086.
52. Zimmermann T, Rietdorf J, Pepperkok R: Spectral imaging and its applications in live cell microscopy. FEBS Letters 2003, 546:87–92. [PubMed: 12829241]
53. Tillberg PW, Chen F, Piatkevich KD, Zhao Y, Yu CC, English BP, Gao L, Martorell A, Suk HJ, Yoshida F, et al.: Protein-retention expansion microscopy of cells and tissues labeled using standard fluorescent proteins and antibodies. Nat Biotechnol 2016, 34:987–992. [PubMed: 27376584]
54. Asano SM, Gao R, Wassie AT, Tillberg PW, Chen F, Boyden ES: Expansion Microscopy: Protocols for Imaging Proteins and RNA in Cells and Tissues. Curr Protoc Cell Biol 2018, 80:e56. [PubMed: 30070431]
55. Gao R, Asano SM, Upadhyayula S, Pisarev I, Milkie DE, Liu TL, Singh V, Graves A, Huynh GH, Zhao Y, et al.: Cortical column and whole-brain imaging with molecular contrast and nanoscale resolution. Science 2019, 363.
56. Li T, Huang S, Zhao X, Wright DA, Carpenter S, Spalding MH, Weeks DP, Yang B: Modularly assembled designer TAL effector nucleases for targeted gene knockout and gene replacement in eukaryotes. Nucleic Acids Res 2011, 39:6315–6325. [PubMed: 21459844]

57. Jinek M, Chylinski K, Fonfara I, Hauer M, Doudna JA, Charpentier E: A Programmable Dual-RNA–Guided DNA Endonuclease in Adaptive Bacterial Immunity. Science 2012, 337:816. [PubMed: 22745249]

58. Zhang FC L; Lodato S; Kosuri S; Church GM; Arletta P;: Efficient construction of sequence-specific TAL effectors for modulating mammalian transcription. Nature Biotechnology 2011, 29:149–153.

59. Voss S, Klewer L, Wu YW: Chemically induced dimerization: reversible and spatiotemporal control of protein function in cells. Curr Opin Chem Biol 2015, 28:194–201. [PubMed: 26431673]

60. Khamo JS, Krishnamurthy VV, Sharum SR, Mondal P, Zhang K: Applications of Optobiology in Intact Cells and Multicellular Organisms. J Mol Biol 2017, 429:2999–3017. [PubMed: 28882542]

61. von Appen A, Kosinski J, Sparks L, Ori A, DiGuilio AL, Vollmer B, Mackmull MT, Banterle N, Parca L, Kastritis P, et al.: In situ structural analysis of the human nuclear pore complex. Nature 2015, 526:140–143. [PubMed: 26416747]

62. Szymborska A, de Marco A, Daigle N, Cordes VC, Briggs JA, Ellenberg J: Nuclear Pore Scaffold Structure Analyzed by Super-Resolution Microscopy and Particle Averaging. Science 2013, 341:655–658. [PubMed: 23845946]

63. Westphal V, Rizzoli SO, Lauterbach MA, Kamin D, Jahn R, Hell SW: Video-rate far-field optical nanoscopy dissects synaptic vesicle movement. Science 2008, 320:246–249. [PubMed: 18292304]

Highlights

- MINFLUX microcopy achieves orders of magnitude better spatial and temporal resolution than camera-based, single-molecule localization and tracking microscopy.
- FLINC biosensors enable super-resolution optical fluctuation imaging of biomolecular localization and activity in living cells.
- DNA - and RNA-based labeling approaches enable multiplexed single-molecule localization microscopy of hundreds of different proteins or RNA transcripts.
- Adaptive optics (AO)-corrected lattice-light sheet microscopy achieves non-invasive live-cell imaging in intact tissues and animals at unprecedented spatiotemporal resolution.

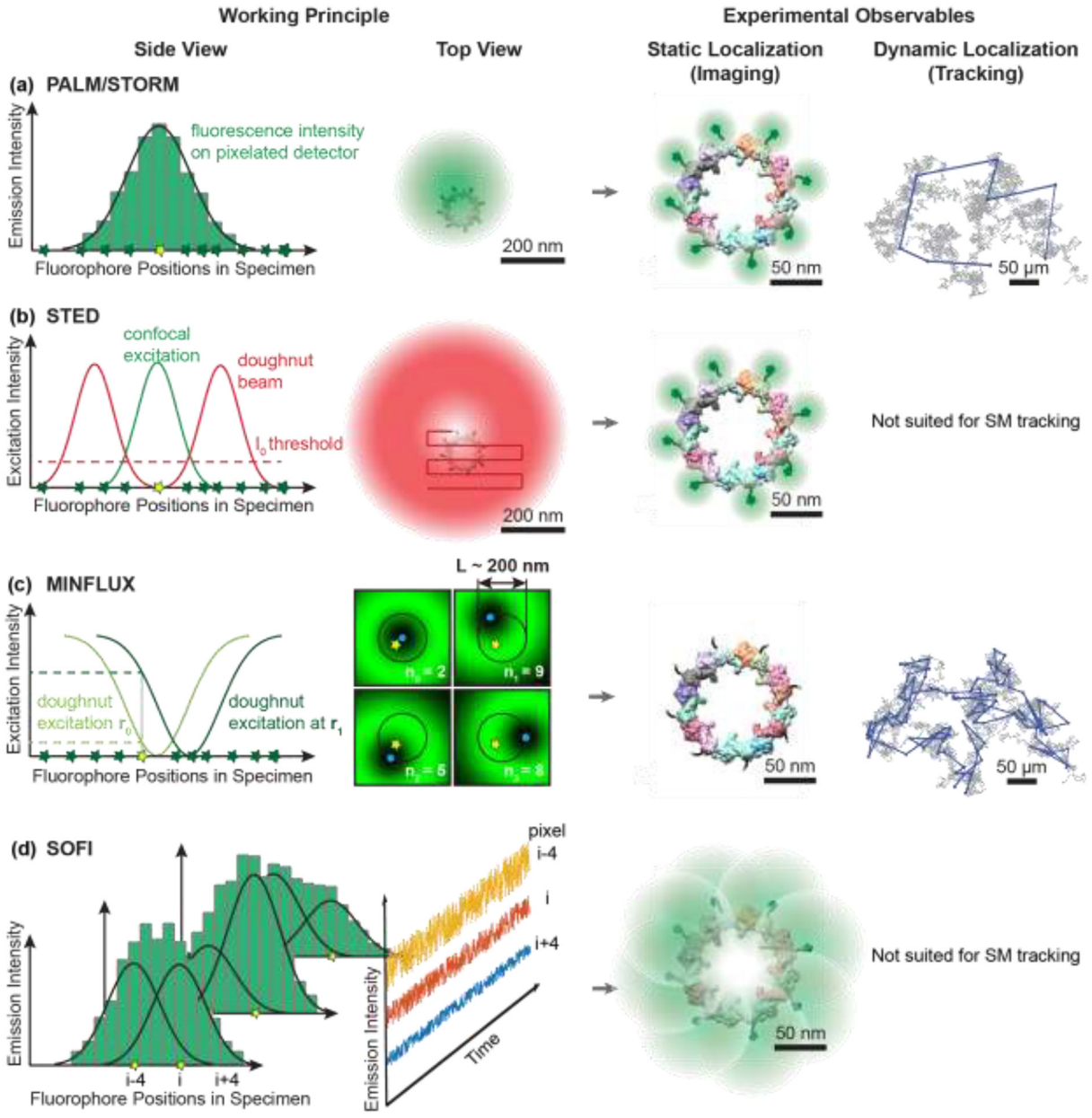

Figure 1. Working principles of selected super-resolution imaging modalities and their resolving capabilities.

a) In coordinate-stochastic (F)PALM/STORM microscopy, fluorophores randomly switch between fluorescence ON and OFF states (yellow and green stars, respectively) when illuminated by wide-field excitation light, resulting in isolated fluorescence signals on the detector. The positions of individual molecules are determined by fitting the pixelated (diffraction-limited) single-molecule images (green histogram) with a mathematical model (black line). Localization precisions of 20–80 nm are routinely achieved for camera-based single-molecule imaging in living cells as indicated by the green probability densities. If a molecule emits photons during several camera frames, its position can be determined at subsequent time points in single-molecule tracking applications, as indicated by the blue

displacements overlaid on the simulated Brownian diffusion trajectory (grey).**b)** In coordinate-targeted STED microscopy, fluorophores (green and yellow stars) in the specimen are selectively excited by a conventional confocal excitation beam (green) and then forced back to the ground state by a red-shifted doughnut beam (red) through stimulated emission. STED microscopy provides a smaller probing volume compared to confocal microscopy, because only the fluorophores near the center of the doughnut beam (below the I_0 intensity threshold for stimulated emission, dashed line) are allowed to remain in the excited state and fluoresce (yellow star). A super-resolved image is acquired pixel-by-pixel by scanning the excitation beam and the overlapping STED doughnut through the sample. STED can achieve a resolution of 20–50 nm in whole-cell imaging, as indicated by the green fluorescence signals overlaid on fluorescently-labeled nucleoporin proteins of the nuclear pore complex [61,62]. The deterministic scanning pattern of STED is not suited for single-molecule tracking; nevertheless, tracking of synaptic vesicles labeled with multiple fluorophores has been demonstrated [63]. **c)** MINFLUX microscopy is a hybrid of coordinate-targeted and coordinate-stochastic microscopy. Wide-field illumination is used to randomly photoactivate a single fluorophore in the specimen, and then a doughnut beam is targeted to four predefined coordinates (blue dots) around the fluorophore. If the fluorophore is located near the intensity minimum, it will only emit a few fluorescence photons, and any small displacement of the doughnut will cause it to emit more photons. The position of the fluorescence emitter can be calculated from the number of photons emitted at the four targeted coordinates (n_0, n_1, n_2, n_3). Localization precisions of 2 nm can be achieved for MINFLUX single-molecule imaging, as indicated by the green probability densities, and 20–50 nm for MINFLUX single-molecule tracking in living cells, as indicated by the blue displacements. **d)** SOFI relies on stochastic fluctuations of fluorescence emitters that independently transition between fluorescent and non-fluorescent states over time. If these emitters are positioned closer than the diffraction limit, then the signal in a given pixel (i-4, i, or i+4) is the sum of the fluorescence signals (overlapping Gaussian profiles) of multiple emitters (yellow stars). Due to fluorophore blinking, the intensity measured in each pixel fluctuates in time (blue, red, and yellow profiles). Computing the nth-order auto- and cross-cumulants of the temporal fluctuations in each pixel can provide resolution improvements by up to a factor of n. Resolutions on the order of 100 nm are routinely achieved in living cells, as indicated by the green probability densities.

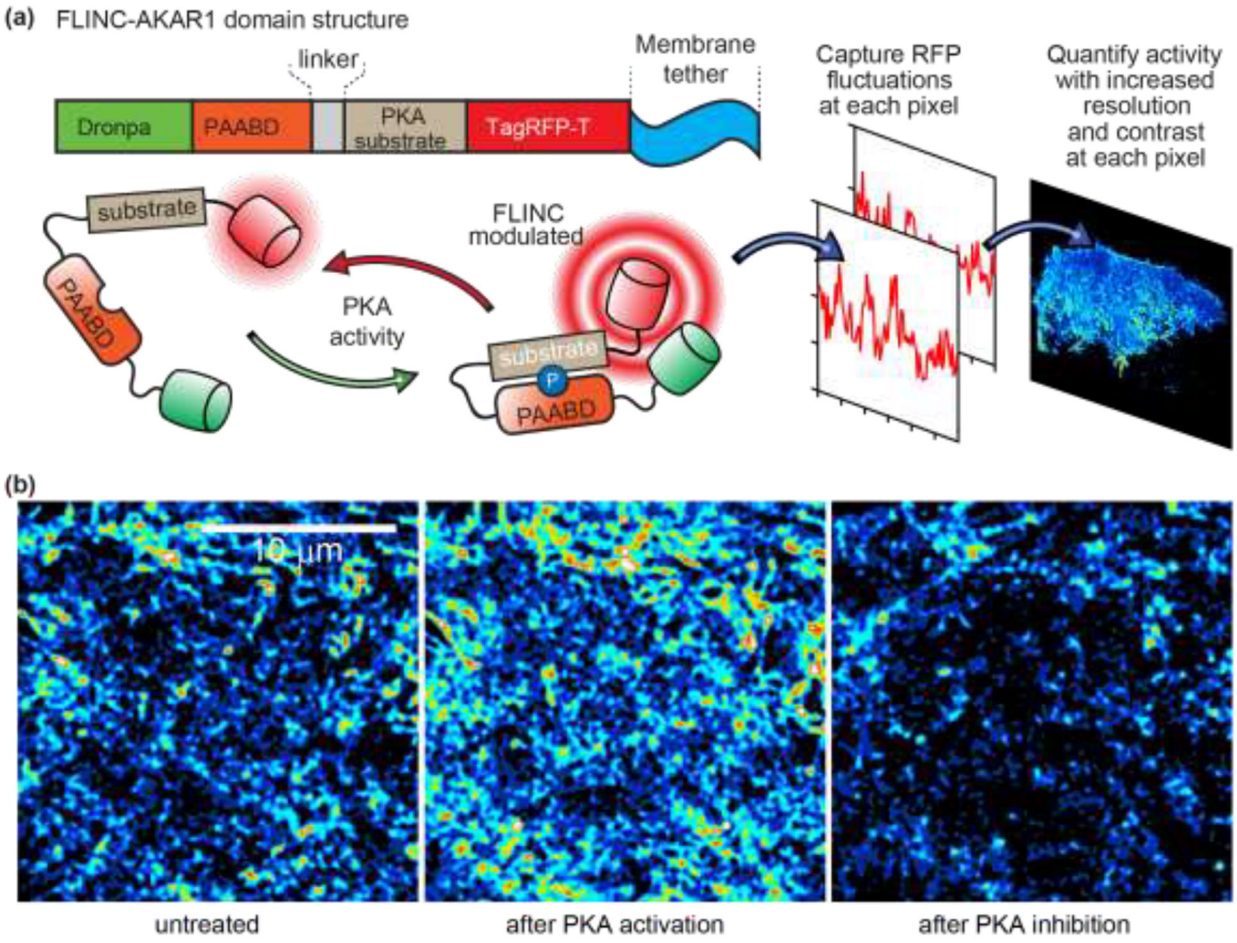

Figure 2. Working principle of the membrane-tethered FLINC–AKAR1 biosensor for photochromic Stochastic Optical Fluctuation Imaging (pcSOFI).

a) The phosphoamino-acid binding domain (PAABD) binds to its substrate upon phosphorylation by PKA, which brings TagRFP-T (red cylinder) into close proximity to Dronpa (green cylinder). The resulting changes in the fluorescence fluctuations kinetics of TagRFP-T provide a quantifiable FLINC signal of the phosphorylation state of the biosensor. **b)** SOFI images of FLINC–AKAR1 biosensors on the plasma membrane of live HeLa cells. After normalization to account for variability in biosensor concentration, the intensity in each pixel is the local FLINC signal, which reports on the local PKA activity. The normalized SOFI images show that PKA activity is spatially localized into distinct micro-domains (left image), and that PKA activity increases upon chemical activation (middle image) and decreases upon chemical inhibition (right image). Figure reproduced and adapted with permission from Ref. [22].

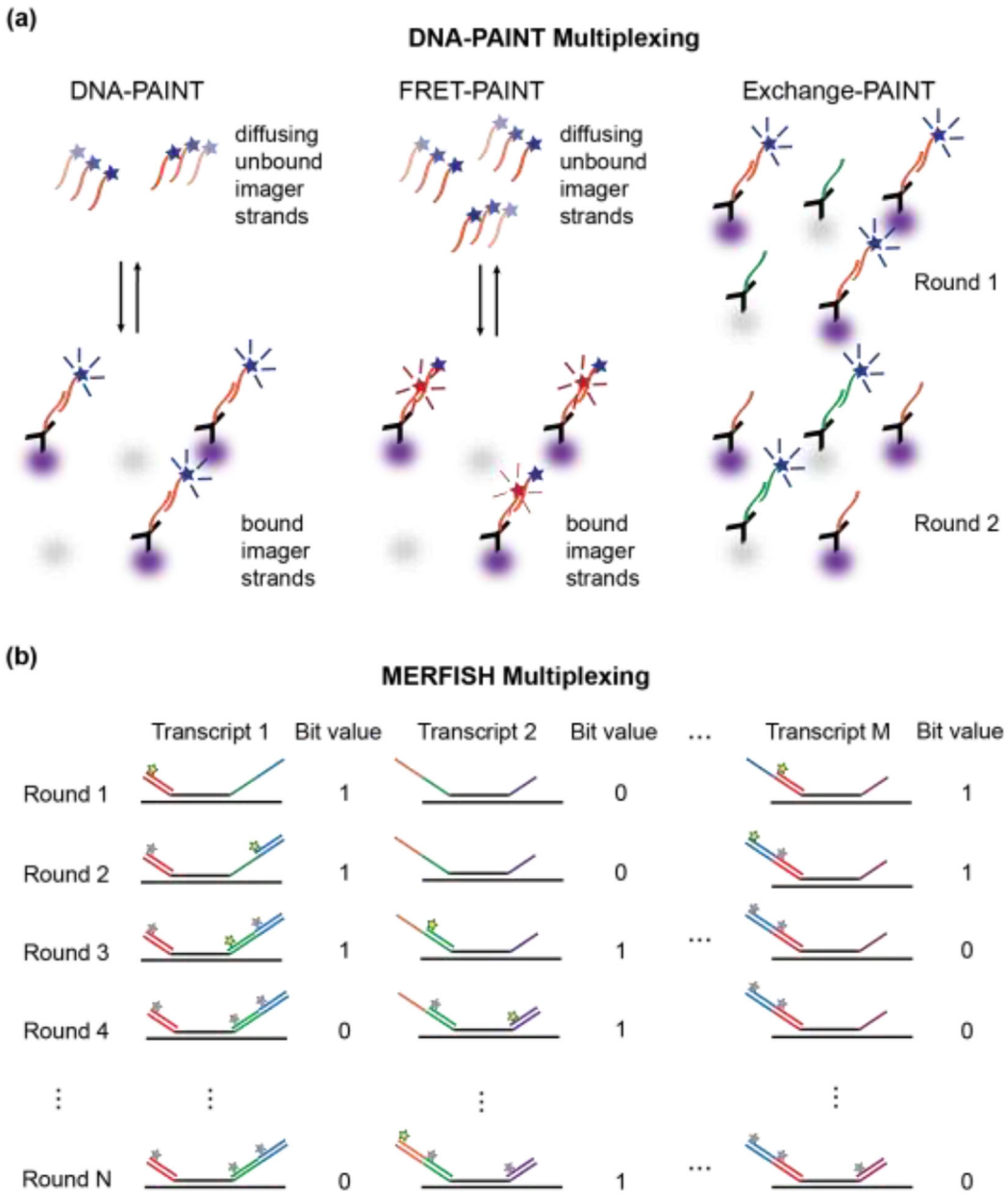

Figure 3. High-content super-resolution microscopy labeling techniques.

a.) DNA-PAINT is used to localize antibody-labeled proteins (purple and gray). Left Panel: Diffusing dye-conjugated imager strands can bind to complementary docking strands on the antibodies. Upon binding, their fluorescence images on the detector become localized in space, which enables precise position estimations of the so-labeled proteins. Middle Panel: Docking strands used in FRET-PAINT are conjugated to a FRET acceptor dye. FRET occurs only after binding of an imager strand, which is conjugated to a FRET donor dye. FRET emission of the acceptor dye is used to localize the labeled protein. Raising the concentration of imager strands does not increase the background in the emission channel of the acceptor dye, but accelerates the data acquisition time by increasing the imager strand binding rates. Right Panel: Exchange-PAINT enables multiplexed labeling by sequentially

introducing multiple different imager strands that are conjugated with the same dye after repeated washing steps. **b)** MERFISH localizes multiple RNA transcripts by introducing encoding RNA probes that bind to M distinct RNA transcripts through complementary base-pairing (black lines). Each encoding probe contains a unique combination of readout sequences (colored lines), which act as docking sites for STORM dye-modified imager probes. Fluorescent imager probes (yellow stars) are sequentially introduced, imaged, and then photobleached or chemically cleaved (grey stars) prior to the next round of imaging. If a localized fluorescence signal is measured in a given imaging round, the position of the RNA transcript can be determined and the bit value for this position is set to 1. Over N rounds of imaging, an N-bit barcode is generated that uniquely identifies the RNA transcript.

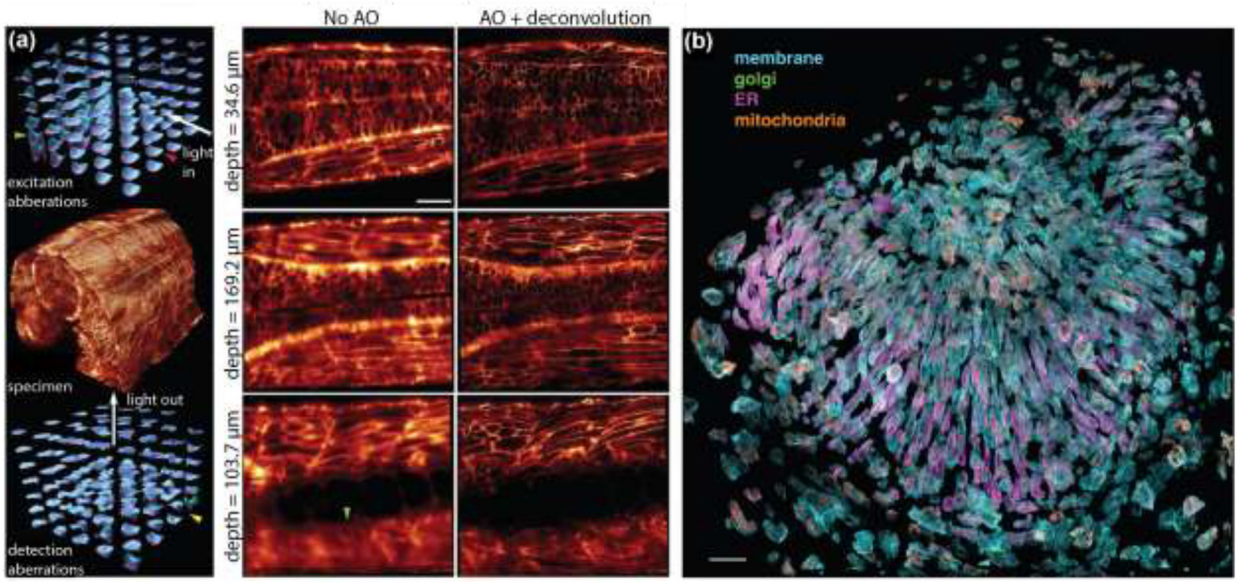

Figure 4. Adaptive optics corrected lattice-light sheet microscopy (AO-LLSM) enables live-cell imaging in whole animals.

(a) Left Panel: Imaging a 170 μm x 185 μm x 135 μm volume in the spine of a zebrafish embryo (center) at diffraction-limited resolution requires local adaptive optics correction of specimen-induced aberrations. Shown are the tiled correction wavefronts applied in the excitation (top) and emission (bottom) light paths. Larger amplitudes of the correction wavefronts are indicative of larger specimen-induced aberrations that occur at greater imaging depths. Right Panel: Slices through the image volume at different imaging depths. There is notable improvement in resolution after adaptive optics correction and deconvolution of images. Scale bar: 30 μm. **b)** Exploded view of hundreds of individual cells in the zebrafish eye. Four different cellular components were simultaneously labeled. The plasma membrane was labeled with a genetically-targeted citrine, the trans-Golgi apparatus was labeled with genetically-targeted mNeonGreen, the endoplasmic reticulum was labeled with genetically-targeted tagRFPt, and mitochondria were labeled with the organelle specific dye MitoTracker Deep Red. Scale bar: 30 μm. Figures reproduced and adapted with permission from Ref. [49].